Archimedean spiral cavity ring resonators in silicon as ultra-compact optical comb filters

Dan-Xia Xu*, André Delâge, Ross McKinnon, Martin Vachon, Rubin Ma, Jean Lapointe, Adam Densmore, Pavel Cheben, Siegfried Janz and Jens H. Schmid

Institute for Microstructual Sciences, National Research Council Canada,
1200 Montreal Road, Ottawa, Canada K1A 0R6.
**Danxia.Xu@nrc-cnrc.gc.ca*

Abstract: We present an ultra-compact comb filter using an add-drop ring resonator with an Archimedean spiral cavity. The cavity consists of two interleaved spiral branches which are connected in the center using arcs of circle of a radius that causes minimum bend loss. We describe the design procedure and examine the physical parameters governing the resonator performance. As an example, we demonstrate experimentally a comb filter with a 25 GHz channel spacing made of silicon photonic wires and only occupies an area of 80 × 90 μm^2, approximately a 70 fold size reduction compared to a racetrack resonator. The filter transmission is free of spurious reflections, attesting to the smooth transition between different sections of the resonator cavity. Over a 40 channel wavelength span, the filter exhibits a quality factor Q > 35,000, extinction ratios > 10 dB, and an excellent power uniformity with variations < 0.5 dB for both the through and drop ports.

OCIS codes: (130.3120) Integrated optics devices; (130.7408) Wavelength filtering devices; (230.5750) Resonators; (230.7390) Waveguides, planar; (060.1810) Buffers, couplers, routers, switches, and multiplexers.

References and links

1. W. Tomlinson, "Evolution of passive optical component technologies for fiber-optic communication systems," J. Lightwave Technol. **26**(9), 1046–1063 (2008).
2. G. Sun, D. S. Moon, A. Lin, W. T. Han, and Y. Chung, "Tunable multiwavelength fiber laser using a comb filter based on erbium-ytterbium co-doped polarization maintaining fiber loop mirror," Opt. Express **16**(6), 3652–3658 (2008).
3. Q. Wu, H. Chan, P. Chu, C. Yu, and D. Hand, "Compact tunable three-dimensional polymer optical waveguide comb filter," Opt. Commun. **277**(1), 89–92 (2007).
4. J. Berthold, A. Saleh, L. Blair, and J. Simmons, "Optical networking: Past, present, and future," J. Lightwave Technol. **26**(9), 1104–1118 (2008).
5. R. Beausoleil, P. Kuekes, G. Snider, S. Wang, and R. Williams, "Nanoelectronic and nanophotonic interconnect," Proc. IEEE **96**(2), 230–247 (2008).
6. A. Shacham, K. Bergman, and L. Carloni, "On the design of a photonic network-on-chip," (IEEE Computer Society Washington, DC, USA, 2007), pp. 53–64.
7. B. Lee, A. Biberman, P. Dong, M. Lipson, and K. Bergman, "All-optical comb switch for multiwavelength message routing in silicon photonic networks," IEEE Photon. Technol. Lett. **20**(10), 767–769 (2008).
8. P. Dong, S. F. Preble, and M. Lipson, "All-optical compact silicon comb switch," Opt. Express **15**(15), 9600–9605 (2007).
9. D. Wang, F. Tong, X. Fang, W. Jin, P. Wai, and J. Gong, "Multiwavelength erbium-doped fiber ring laser source with a hybrid gain medium," Opt. Commun. **228**(4-6), 295–301 (2003).
10. S. Bidnyk, A. Balakrishnan, A. Delage, Mae Gao, P. A. Krug, P. Muthukumaran, and M. Pearson, "Planar comb filters based on aberration-free elliptical grating facets," J. Lightwave Technol. **23**(3), 1239–1243 (2005).
11. A. Densmore, S. Janz, R. Ma, J. H. Schmid, D. X. Xu, A. Delâge, J. Lapointe, M. Vachon, and P. Cheben, "Compact and low power thermo-optic switch using folded silicon waveguides," Opt. Express **17**(13), 10457–10465 (2009).
12. D.-X. Xu, A. Densmore, A. Delâge, P. Waldron, R. McKinnon, S. Janz, J. Lapointe, G. Lopinski, T. Mischki, E. Post, P. Cheben, and J. H. Schmid, "Folded cavity SOI microring sensors for high sensitivity and real time measurement of biomolecular binding," Opt. Express **16**(19), 15137–15148 (2008).
13. S. Chu, B. Little, W. Pan, T. Kaneko, S. Sato, and Y. Kokubun, "An eight-channel add-drop filter using vertically coupled microring resonators over a cross grid," IEEE Photon. Technol. Lett. **11**(6), 691–693 (1999).

#120774 - $15.00 USD Received 1 Dec 2009; revised 6 Jan 2010; accepted 9 Jan 2010; published 15 Jan 2010

14. D. Rezzonico, A. Guarino, C. Herzog, M. Jazbinsek, and P. Gunter, "High-finesse laterally coupled organic-inorganic hybrid polymer microring resonators for VLSI photonics," IEEE Photon. Technol. Lett. **18**(7), 865–867 (2006).
15. J. Heebner, R. Grover, and T. Ibrahim, *Optical microresonators: theory, fabrication, and applications* (Springer Verlag, 2007).
16. D.-X. Xu, A. Densmore, P. Waldron, J. Lapointe, E. Post, A. Delâge, S. Janz, P. Cheben, J. H. Schmid, and B. Lamontagne, "High bandwidth SOI photonic wire ring resonators using MMI couplers," Opt. Express **15**(6), 3149–3155 (2007).
17. W. R. McKinnon, D.-X. Xu, C. Storey, E. Post, A. Densmore, A. Delâge, P. Waldron, J. H. Schmid, and S. Janz, "Extracting coupling and loss coefficientsfrom a ring resonator," Opt. Express **17**(21), 18971–18982 (2009).

1. Introduction

Optical comb filters and switches are essential components for wavelength selection and transmission control of photonic signals in many applications [1–4]. For example, optical interconnects built using silicon photonics has emerged as a viable technology for transporting high data flow between computer chips [5,6]. This technology requires compact switches capable of operating over a wide wavelength range for routing multiwavelength data. As a transmission control element, a comb switch can be used to direct a large group of optical data channels to selected destinations, facilitating parallel data processing architectures [1,7,8]. Another example is multi-wavelength lasers for WDM communication systems, optical sensing and metrology that use comb filters as external filters in conjunction with broadband gain media such as Er^{+} doped fibers or semiconductor optical amplifiers [1,2]. Being separated from the active gain media, these comb filters can be optimized and temperature stabilized separately and are free from constraints imposed on internal filters.

There have been many implementations of comb filters reported in the literature, and integrated planar waveguide filters include devices based on Mach-Zehnder interferometers [9], echelle gratings [10] and add-drop ring resonators. Even though ring resonators are considered compact compared to other devices, a comb filter with a 50 GHz spacing using a conventional racetrack resonator made of silicon photonic wires (cross-section dimensions of 250 nm × 500 nm) still occupies an area of 400 μm × 400 μm. This is the design used in a recent demonstration of simultaneous all-optical switching of 20 wavelength channels in a ring resonator based 1 × 2 comb switch [7,8]. A smaller device size would facilitate a higher level of integration and reduce the power consumption for base point control and switching [11], which is a key consideration in optical interconnects.

Here we report a new configuration of ultra-compact comb filters based on silicon photonic wire add-drop ring resonators having an Archimedean spiral cavity, where the drop-port provides a comb filter response. Owning to the high refractive index of silicon, photonic wires can be folded into a tight spiral with a minimum bend radius of only a few micrometers. We have previously reported the first implementation of a spiral cavity resonator in all-pass configuration for biosensing applications [12]. We showed that the use of a spiral is an effective way of increasing the cavity length within a small area, leading to increased resonator quality factor Q and relaxed critical coupling tolerances for obtaining a high resonance extinction ratio. This feature increases the manufacturing tolerance of the resonators, which is an important consideration for sensor arrays. In this paper, we demonstrate that the Archimedean spiral design lends itself equally well to the add-drop configuration, forming highly compact comb filters with small channel spacing. Furthermore, we show that placing the drop-port coupler closely 'down stream' from the through port improves the power coupled to the drop-port. We describe the design approach to limit the bend radiation loss and avoid unwanted reflections in the cavity, and conduct a systematic investigation on the design parameters that govern the resonator performance. A high performance comb filter made of silicon photonic wires with a 25 GHz channel spacing and a size of only 80 × 90 μm^2 is experimentally demonstrated. Together with the ability to engineer dispersion in silicon photonic wires, this type of ultra-compact filter provides considerable advantages for many applications.

#120774 - $15.00 USD Received 1 Dec 2009; revised 6 Jan 2010; accepted 9 Jan 2010; published 15 Jan 2010

2. Spiral cavity ring resonator design

An Archimedean spiral has equal spacing between successive turns, and offers the highest filling ratio among different spiral varieties for a given waveguide separation. A SEM image of a spiral cavity resonator is shown in Fig. 1a, and a schematic layout of the cavity center portion is shown in Fig. 1b. The cavity consists of two interleaved symmetrical Archimedean spirals joined in the center by two arcs of circle and externally by input and output waveguides and directional couplers. As a function of angle θ, the midpoint of the two spiral waveguide branches can be defined with the following relations:

$$R_s(\theta) = (S_w / \pi)\theta, \qquad \theta > 0 \tag{1a}$$

$$x_{1,2} = \pm R_s \cos\theta, \qquad y_{1,2} = \mp R_s \sin\theta \tag{1b}$$

where S_w is a pre-chosen waveguide separation. The radius of curvature of the spiral is $R_C = (S_w / \pi)\left(1+\theta^2\right)^{3/2} / \left(2+\theta^2\right)$, such that the minimum radius at the center ($\theta = 0$) is $S_w/2\pi$. This value is usually lower than the practical minimum radius of curvature R_{min} for silicon photonic wires (typically $R_{min} > 2$ μm). To eliminate the spiral section where the curvature is too small, we use circular arcs of radius R_{min} in the center to connect the spiral branches. In order to avoid reflection and scattering points, the waveguide tangential direction needs to maintain continuity, so the arc must have the same slope as the spiral at the connecting point (at an angle of θ_{min} as shown in Fig. 1b). For reasons of symmetry, the arc must also pass the origin (0, 0).

Using these two conditions, the value of θ_{min} and the center location (x_0, y_0) of the arc can be determined as follows:

$$\theta_{\min} = \sqrt{4\pi^2 R_{\min}^2 / S_w^2 - 1}, \tag{2a}$$

$$x_0 = \frac{S_w}{2\pi}\cos\theta_{\min}\left(\theta_{\min} - \tan\theta_{\min}\right), \tag{2b}$$

$$y_0 = \frac{S_w}{2\pi}\cos\theta_{\min}\left(\theta_{\min}\tan\theta_{\min} + 1\right). \tag{2c}$$

To accommodate the second coupler in the add-drop configuration, a straight (vertical) section is included at the end of the spiral before joining it to the horizontal coupler section using an arc.

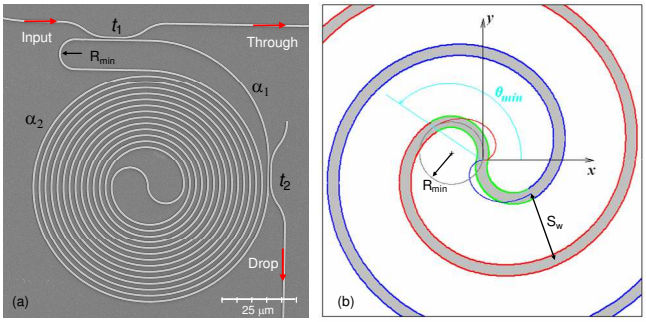

Fig. 1 (a) SEM image of an Archimedean spiral cavity add-drop ring resonator (Ring F in Table 1). Here α_1 is the field loss factor incurred between the two couplers, and α_2 is the loss factor for the rest of the cavity length. (b) Center portion of the resonator cavity, where the red and blue outlined sections indicate the two interleaved Archimedean spiral waveguides, joined in the center by two arcs of circle (outlined in green) of radius R_{min}. The red and blue single lines are the part of the spiral not used in the cavity. The waveguide center-to-center separation is Sw.

#120774 - $15.00 USD Received 1 Dec 2009; revised 6 Jan 2010; accepted 9 Jan 2010; published 15 Jan 2010

Directional coupler(s) are used in conjunction with the cavity to form all-pass or add-drop resonators. The drop-port coupler has typically been placed at the half-length point of the cavity, although earlier work has also demonstrated resonators with vertical or in-plane couplers placed orthogonal to each other along a circular cavity [13,14]. Considering the general case where the two couplers are placed asymmetrically along the cavity (see Fig. 1a), each section incurring a propagation loss with a field amplitude loss factor of α_1 and α_2 (so that $\alpha = \alpha_1 \alpha_2$ is the total cavity field loss factor), we have derived that the transmission of the through-port (I_T) and drop-port (I_D) can be expressed as:

$$I_T = \frac{t_1^2 - 2\alpha t_1 t_2 \cos\phi + (\alpha t_2)^2}{1 - 2\alpha t_1 t_2 \cos\phi + (\alpha t_1 t_2)^2}, \tag{3a}$$

$$I_D = \frac{(1-t_1^2)(1-t_2^2)\alpha_1^2}{1 - 2\alpha t_1 t_2 \cos\phi + (\alpha t_1 t_2)^2}. \tag{3b}$$

Here t_1 and t_2 are the self-coupling coefficients for the through and drop port couplers, respectively, φ is the phase, and the couplers are assumed to be lossless. When the drop-port coupler is at the half-length point of the cavity as it is often the case, $\alpha_1 = \alpha_2 = \sqrt{\alpha}$ and Eq. (3b) returns to the more familiar form reported in the literature [15]. When the drop-port is very close to the through-port, the loss factors can be approximated as $\alpha_1 \approx 1$ and $\alpha_2 \approx \alpha$, and I_D is increased according to Eq. (3b). For this reason, we place the drop-port coupler closely 'down stream' from the through-port as shown in Fig. 1a.

3. Experiments and discussions

We first investigate the contributions of the minimum radius R_{min}, waveguide separation S_w and cavity length L on device performance using all-pass resonators, followed by the implementation of add-drop filters. Devices were fabricated on silicon-on-insulator (SOI) wafers having a 260 nm thick silicon layer on a 2 μm thick buried oxide layer. Both the bus and cavity waveguides are 450 nm wide, patterned by electron-beam lithography and plasma etching. Fabrication details have been reported previously [12,16]. In order to improve the waveguide to fiber coupling efficiency as well as to minimize the Fabry-Perot reflections from the waveguide facets, inverse taper mode size converters with a width of 150 nm and covered in an SU8 polymer overclad were adopted, while the resonators are exposed to air. Table 1 summarizes R_{min}, L, device area and the free-spectral-range (FSR) at a wavelength of λ = 1550 nm for the resonators reported here. All resonators have directional couplers with a 5 μm long straight section, a gap distance of 0.4 μm for Rings A–E, and 0.36 and 0.4 μm for the through and drop ports of Ring F respectively. The spiral waveguide (center-to-center) separation S_w of 2 μm and 10 μm were tested, and we found that the resonators performed similarly, indicating that there is no adverse effect in using S_w as small as 2 μm. All the examples discussed below use a value of S_w = 2 μm. These resonators were designed to operate in TM polarization, since the all-pass resonators were also used as biosensors for which the TM mode provides a higher sensitivity than TE [12]. The spiral configuration can be easily applied to resonators for TE polarization as well, requiring only the adjustment of coupler strengths.

Table 1. Spiral resonator minimum radius R_{min} for the center arc of circle, cavity length L, device area and the FSR at a wavelength of 1550 nm, for all-pass resonators A–E and add-drop resonator F.

Sample	Ring A	Ring B	Ring C	Ring D	Ring E	Ring F
R_{min} (μm)	5	5	5	2	2	5
L (μm)	430	700	1350	417	700	2400
Cavity area (μm^2)	35 × 55	45 × 45	60 × 70	35 × 45	45 × 45	80 × 90
FSR (nm)	1.16	0.72	0.37	1.19	0.71	0.23

#120774 - $15.00 USD Received 1 Dec 2009; revised 6 Jan 2010; accepted 9 Jan 2010; published 15 Jan 2010

Optical testing was performed using a tunable laser connected to a polarization controller to select TM polarization as the input, then fiber-coupled to the waveguide via a polarization maintaining lensed fiber. The output light was collected and focused onto a photodetector using a 20 × objective lens. The laser wavelength scanning range is λ = 1470 nm – 1580 nm, and a scan step of ≤ 1 pm was used. Figure 2 shows the transmission spectra for all-pass resonators Ring A and C, with an FSR of 1.09 nm and 0.35 nm at λ = 1520 nm, and footprints of 35 × 45 μm^2 and 60 × 70 μm^2, respectively. Note these FSR values are smaller than that listed in Table 1 for λ = 1550 nm due to waveguide dispersion and the dependence of FSR on λ. No spurious features are found in the device transmission spectra over the entire laser scan range, indicating smooth transitions between different sections of the resonant cavity. The quality factors Q are approximately 33,000 and 74,000 at these wavelengths for Ring A and C, respectively.

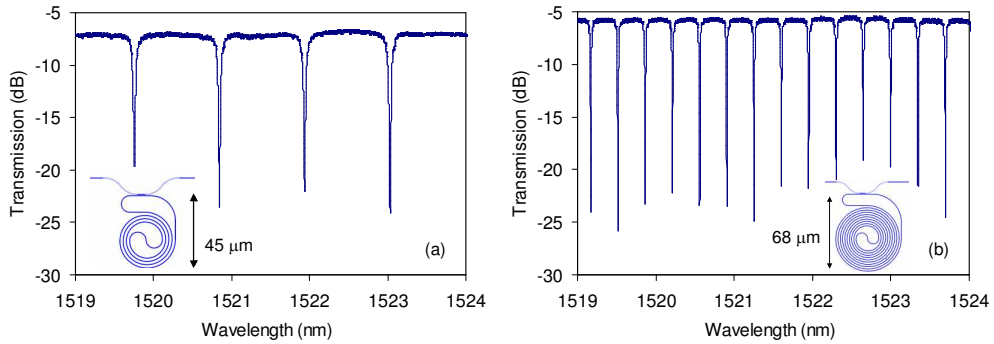

Fig. 2. Transmission spectra of all-pass resonators (a) Ring A with L = 430 μm and a FSR of 1.09 nm at λ = 1520 nm; (b) Ring C with L = 1350 μm and a FSR of 0.35 nm.

Resonator performance is primarily determined by the coupling coefficients and cavity loss factor. We have previously demonstrated that α and t can be extracted from an all-pass resonator spectrum and unambiguously distinguished based on their wavelength dependence [17]. In this study, the extracted values are assigned as α or t relying on the fact that t should be similar for Rings A–E since they have the same couplers. The self-coupling coefficient t is shown in Fig. 3a as a function of wavelength. Data from all five resonators closely overlap each other, indicating good dimensional reproducibility of these devices. The values of t decrease with λ closely following a sinusoidal function, due to the mode size expansion with λ leading to increased modal-overlap in directional couplers.

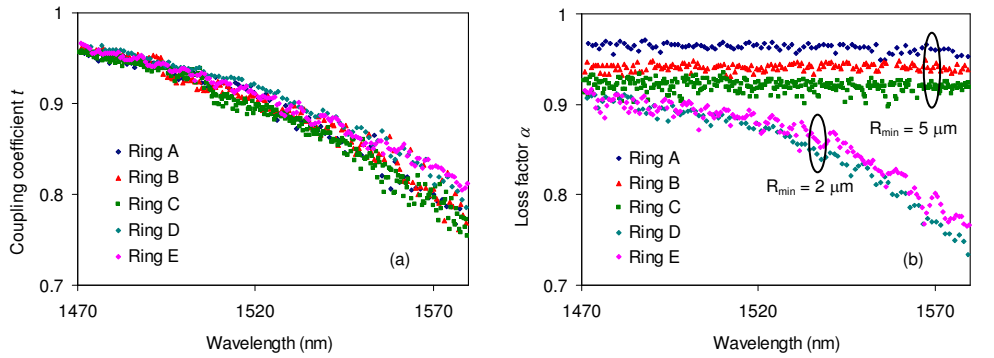

Fig. 3. (a) Extracted coupling coefficient t for Ring A – E which have varied cavity length L and minimum bend radius R_{min} of 2 and 5 μm, but the same couplers.; (b) Corresponding field loss factor α.

#120774 - $15.00 USD Received 1 Dec 2009; revised 6 Jan 2010; accepted 9 Jan 2010; published 15 Jan 2010

The loss factors for Rings A–E are shown in Fig. 3b. We observe that for Rings A–C with R_{min} = 5 μm, α is independent of λ while it decreases linearly with L, suggesting that the waveguide propagation loss is the main cavity loss mechanism. A propagation loss of 6 dB/cm is estimated, which is in good agreement with waveguide loss measurements using the cut-back technique. For Rings D and E with R_{min} = 2 μm, α decreases considerably with λ while being almost independent of the cavity length. We attribute the dominating loss mechanisms in Rings D and E to bend radiation loss and mode-mismatch loss at the center of the cavity where the two arcs join with a bend radius discontinuity from $-R_{min}$ to $+ R_{min}$.

The above analysis led us to adopt R_{min} = 5 μm and S_w = 2 μm in our add-drop resonator designs. Ring F is such an add-drop resonator with a cavity length L = 2400 μm, designed to produce a 25 GHz channel spacing (or FSR = 0.2 nm at λ = 1550 nm), since the group index is ~5 for the TM mode in these waveguides. The directional coupler gaps are 0.36 μm and 0.4 μm for the through and drop ports, respectively. A smaller gap in the through-port than that in Rings A–E is used here to accommodate the higher cavity loss in the longer cavity, and the asymmetric coupler strength is used to meet the critical-coupling condition. The device size is $80 \times 90\ \mu m^2$, which is approximately 70 times smaller compared to a conventional racetrack design with the same cavity length. In fact, the spiral section of the resonator area is well approximated by $(LS_w + 4\pi R_{min}^2)$. For large L, the area scales almost linearly with L and the size increase for a device changing the channel spacing from FSR_1 to FSR_2 is proportional to the ratio FSR_1/FSR_2 (in GHz), while racetrack resonators would see the device area increase proportional to $(FSR_1/FSR_2)^2$. Clearly, the size advantage of Archimedean spiral cavity resonators is particularly significant for filters with small channel spacing.

Figure 4 shows the transmission spectra of Ring F for both the add and drop ports, extending over 40 channels with excellent channel power uniformity. Transmission variations are < 0.2 dB for the through port, and < 0.5 dB for the drop port within this 10 nm wavelength range centered at λ = 1575 nm. The ratio between the maximum power at the through and drop port is $\eta = I_T^{max} / I_D^{max} \leq 2.5$dB, which represents the excess loss of the drop channel. Here I_T^{max} is defined as the maximum through-port output power when off-resonance and I_D^{max} is the maximum drop-port power when on-resonance. The extinction ratios ER_T and ER_D exceed 10 dB for both ports, with a quality factor Q > 35,000 in this wavelength range. Over the entire laser scanning range, the resonator behavior does show variations, as represented by the maximum and minimum power shown in Fig. 5a. The highest Q of ~70,000 is obtained at λ ~1470 nm, but the drop power is much lower (η ~10 dB). The factors contributing to these performance variations are analyzed below.

In an add-drop resonator, the drop-port coupler is formally equivalent to a lumped loss that transfers power out of the cavity, such that the 'loss' seen by the through port is $\alpha' = \alpha t_2$. The coefficients α' and t_1 can be extracted from the through port spectrum using the data extraction procedure described earlier. Then α can be calculated from α' if t_2 is known. Based on the results shown in Fig. 3a, there is good reproducibility in coupling coefficients between devices with nominally the same couplers. We therefore assume that the drop-port coupler in Ring F has the same coupling coefficient as that in Ring C, since these two couplers have the same dimensions and were fabricated on the same chip. Figure 5b shows α' and t_1 directly obtained from Ring F, t_2 from Ring C, and the cavity loss calculated from $\alpha = \alpha'/t_2$.

#120774 - $15.00 USD Received 1 Dec 2009; revised 6 Jan 2010; accepted 9 Jan 2010; published 15 Jan 2010

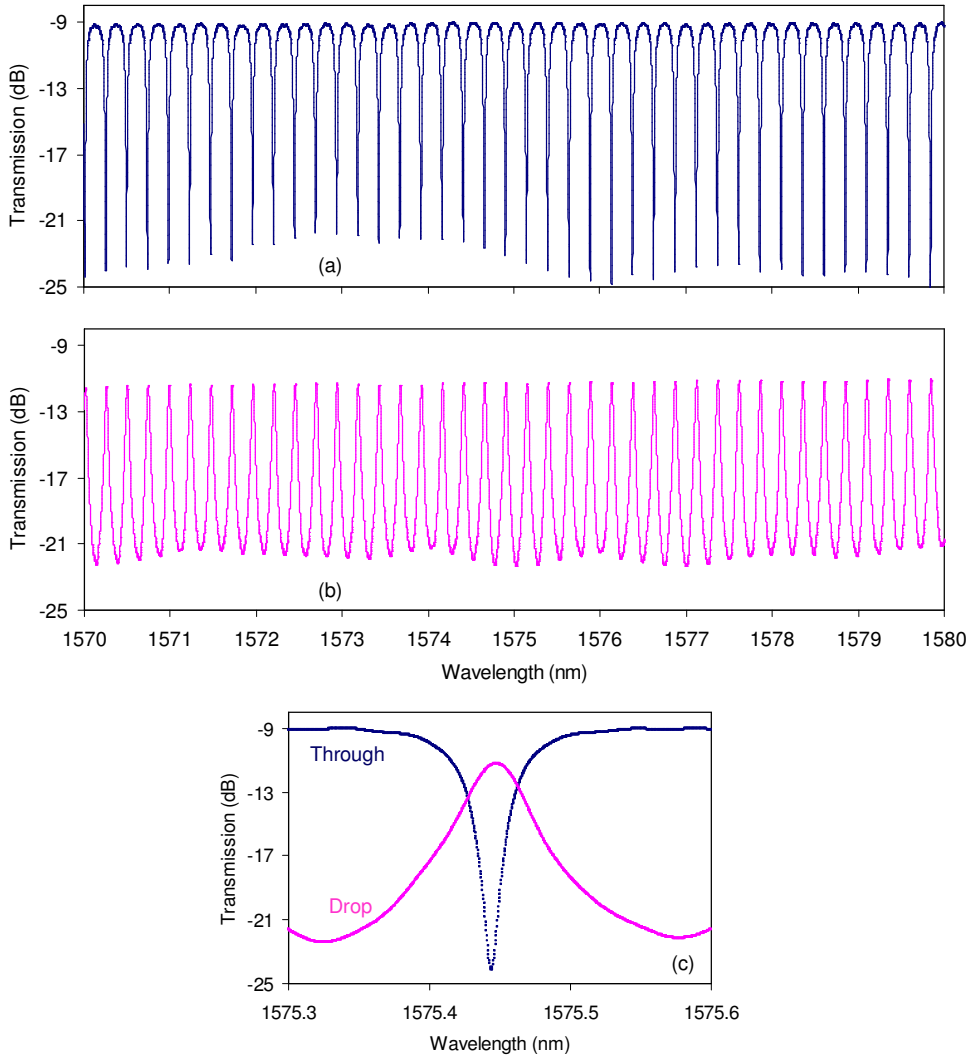

Fig. 4. Measured transmission spectra of add-drop resonator ring F: (a) Through port, (b) Drop port, and (c) Close-up of a single resonance for both ports.

For an ideal add-drop resonator with a lossless cavity, the output power ratio $\eta = 1$ when the two couplers are identical. Generally, there is a non-zero cavity loss, and in this case it is possible to modify η, ER_T and ER_D by adjusting t_1 and t_2. Figure 6 shows the calculated intensity maxima and minima at the two ports, for $t_1 = 0.78$, $\alpha = 0.83$ (the experimental values at $\lambda = 1575$ nm) and $(1 - t_2)$ varying from 0 to 0.4. The through-port maximum power $I_T^{\max}$ is relatively insensitive to the change in t_2 (and t_1), but $I_D^{\max}$ is strongly dependent on both coupling coefficients (see Eq. (3). As $(1 - t_2)$ decreases, both ER_T and ER_D are enhanced but $I_D^{\max}$ decreases, making η larger. On the other hand, when the coupler is made strong enough so that η approaches unity, ER_T and ER_D decrease. To improve all the performance parameters simultaneously, the cavity loss must be reduced.

#120774 - $15.00 USD Received 1 Dec 2009; revised 6 Jan 2010; accepted 9 Jan 2010; published 15 Jan 2010

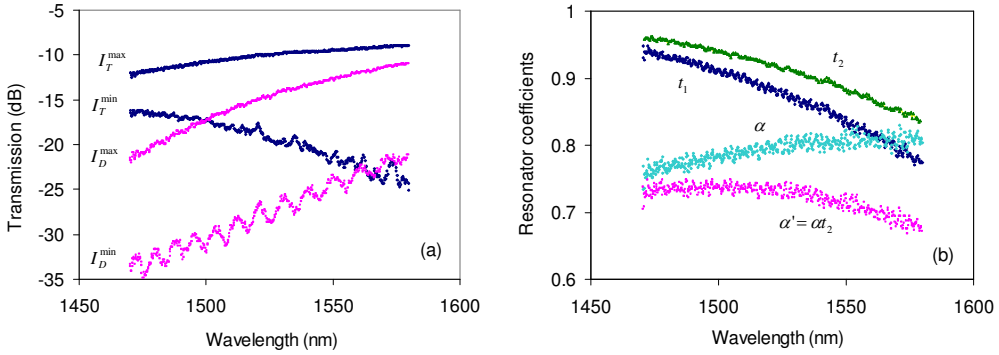

Fig. 5. (a) Measured transmission maxima and minima of the through and drop ports in Ring F. (b) Extracted through-port coupling coefficient t_1 and lumped loss $\alpha' = at_2$ in Ring F, and the equivalent coupling coefficient t_2 that is extracted from Ring C which has the same coupler as the drop port in Ring F.

These results in Fig. 6 explain the resonator experimental behavior shown in Fig. 5a, and the variations of the device outputs approximately matches in trend, although the critical coupling condition ($t_1 = \alpha' = \alpha t_2$) shown in the calculations is not reached in the measurements. As the curves in Fig. 5b shows, a stronger through-port coupler (smaller t_1) is required to reach critical coupling. The increase of $I_D^{\max}$ with λ is mainly caused by the decrease of both t_1 and t_2, since α is only weakly dependent on wavelength. The conditions for the device at λ = 1575 nm correspond to the vertical dashed line in Fig. 6 where $t_2 = 0.84$, and the calculated values are ER_T = 13.7 dB, ER_D = 10.5 dB, and η = 2.04 dB, which are in good agreement with the measurements. If one wishes to optimized the device performance for operating in the C-band (λ = 1530–1565 nm), the self-coupling coefficients should be decreased either by increasing the coupler length or by decreasing the coupler gap. Another point as noted earlier is the advantage of placing the drop-port coupler closely down stream from the through port, so that $\alpha_1 \sim 1$ and $\alpha_2 \sim \alpha$ (see Eq. (3b). By so doing, η is reduced by ~0.8 dB for Ring F discussed here, compared to the hypothetical case of placing the drop-port coupler at half-length point of the cavity.

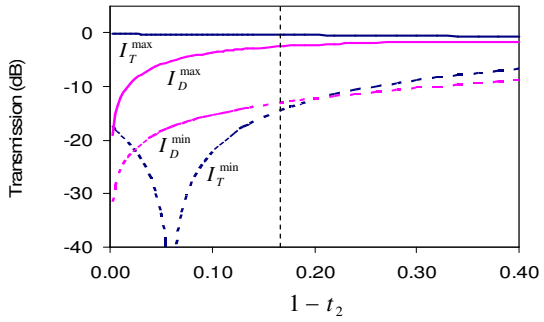

Fig. 6. Calculated transmission maxima and minima in an add-drop resonator as a function of $(1 - t_2)$, using the following parameters: $t_1 = 0.78$ and $a = 0.83$. Dashed vertical line indicates the case for Ring F at λ = 1575 nm where $t_2 = 0.84$.

4. Summary

In this paper we report an ultra-compact comb filter design using an add-drop resonator with an Archimedean spiral cavity. To maintain an acceptable minimum bend radius at the cavity

#120774 - $15.00 USD Received 1 Dec 2009; revised 6 Jan 2010; accepted 9 Jan 2010; published 15 Jan 2010

center, arcs of circle are used to connect two interleaved spiral branches. Design procedures for ensuring continuity in the waveguide tangential directions are described. We have also analyzed the transmission characteristics of resonators with the add- and drop- couplers placed in highly asymmetric locations along the resonator cavity, and the expressions reveal that by placing the drop-coupler closely 'down stream' from the through-coupler, a higher drop power can be achieved. Experimental implementations using silicon wire waveguides demonstrate that the resonator transmissions are free of spurious reflections, and this type of resonators is amendable to a wide range of design parameters in both all-pass and add-drop configurations, as long as the minimum radius is properly chosen. We experimentally demonstrate a comb filter with a ~25 GHz spacing and a footprint of only 7200 μm^2, with excellent power uniformity over a 40 channel wavelength span, and a maximum output power difference between the through and drop ports of less than 2.5 dB. The extinction ratios and the quality factor exceed 10 dB and 35,000, respectively. Furthermore, this spiral design configuration is applicable to other high index contract waveguide systems.

Acknowledgement

The authors gratefully acknowledge the assistance of Jeff Fraser in preparing SEM images.

#120774 - $15.00 USD Received 1 Dec 2009; revised 6 Jan 2010; accepted 9 Jan 2010; published 15 Jan 2010